MITSUBISHI ELECTRIC RESEARCH LABORATORIES
https://www.merl.com

Divert-feasible lunar landing under navigational uncertainty

Lishkova, Yana; Vinod, Abraham P.; Di Cairano, Stefano; Weiss, Avishai

TR2024-174 December 18, 2024

Abstract

We develop a guidance policy for lunar landing under navigational uncertainty with feasible divert in the event a hazard is detected. Offline, we compute stochastic controllable sets under convexified dynamics and constraints that characterize the set of noisy state estimates from which the lander can be driven to a landing site with a pre-specified, sufficiently high probability. We establish that the sets computed for the convexified problem are inner-approximations of the true stochastic controllable sets. The controllable sets are parameterized by available fuel mass and length of trajectory, and provide a tractable method to quickly assess online whether a landing site is reachable. Numerical simulations demonstrate the efficacy of the approach.

2024 Conference on Decision and Control

© 2024 MERL. This work may not be copied or reproduced in whole or in part for any commercial purpose. Permission to copy in whole or in part without payment of fee is granted for nonprofit educational and research purposes provided that all such whole or partial copies include the following: a notice that such copying is by permission of Mitsubishi Electric Research Laboratories, Inc.; an acknowledgment of the authors and individual contributions to the work; and all applicable portions of the copyright notice. Copying, reproduction, or republishing for any other purpose shall require a license with payment of fee to Mitsubishi Electric Research Laboratories, Inc. All rights reserved.

Mitsubishi Electric Research Laboratories, Inc.
201 Broadway, Cambridge, Massachusetts 02139

Divert-feasible lunar landing under navigational uncertainty

Yana Lishkova[1], Abraham Vinod[2], Stefano Di Cairano[2], and Avishai Weiss[2*]

***Abstract*— We develop a guidance policy for lunar landing under navigational uncertainty with feasible divert in the event a hazard is detected. Offline, we compute stochastic controllable sets under convexified dynamics and constraints that characterize the set of noisy state estimates from which the lander can be driven to a landing site with a pre-specified, sufficiently high probability. We establish that the sets computed for the convexified problem are inner-approximations of the true stochastic controllable sets. The controllable sets are parameterized by available fuel mass and length of trajectory, and provide a tractable method to quickly assess online whether a landing site is reachable. Numerical simulations demonstrate the efficacy of the approach.**

I. Introduction

The Moon is seeing a resurgence of activity, and the partial successes and failures of recent missions to the lunar surface have demonstrated that autonomous planetary landing remains challenging [1], [2]. Due to the presence of water ice in the permanently shadowed craters at the south pole of the Moon [3], the south pole has been selected for a future human outpost; landing amidst its rough terrain necessitates increased precision and robustness of powered descent guidance (PDG) algorithms, and the capability to divert from the primary target in case a hazard is detected.

In recent years, fuel-optimal PDG has been an active area of research, see, e.g., [4]–[6], and references therein. In these works, PDG is the solution to an appropriately formulated optimal control problem that is discretized and solved via numerical optimization. Nonlinear lander dynamics and a thrust lower bound render the fuel-optimal PDG problem non-convex. However, under certain assumptions, the non-convex optimal control problem can be solved to global optimality by convex optimization, *losslessly* [6]–[9].

For hazard avoidance, [10] used the lossless convexification approach of [11] to compute *controllable sets*, that is, the set of initial conditions that can reach, or in this case, land at, a specified target. The sets were pre-computed for a range of trajectory lengths and available fuel mass, to be stored onboard the lander. Online, in the event a hazard is detected, the current state of the lander is checked for inclusion against the database of controllable sets at candidate divert sites, providing a real-time feasible method for evaluating the lander's ability to reach a given site.

However, for both the nominal trajectory and the divert maneuvers, there is a challenge in guaranteeing constraint satisfaction, as the lander only knows its state approximately [2]. To the best of the authors' knowledge, no prior work on lossless convexification-based PDG has provided theoretical guarantees for safe landing under navigational uncertainty; see [12], [13] for alternative approaches. In this work, we extend [10] to explicitly account for the uncertainty in position and velocity during powered descent.

The contributions and structure of the paper are as follows. In Section II, we propose a formulation for the fuel-optimal PDG problem under navigational uncertainty, such that the problem constraints are satisfied to user-specified probability. We describe the lander dynamics, model navigational uncertainty as noisy state estimates, and describe the problems of nominal trajectory design and divert capability. In Section III, we develop a tractable approach for trajectory generation. We reformulate the PDG problem as a chance-constrained optimal control problem, where the probability of constraint satisfaction is assured by constraint tightening with respect to a bounded uncertainty set [14], and losslessly convexify the non-convex dynamics and constraints. Additionally, using the convex problem formulation, we develop inner-approximations of stochastic controllable sets, which characterize the set of noisy state estimates from which the lander can be driven to a landing site with user-specified probability. As in [10], these stochastic controllable sets are then used for real-time assessment of the reachability of alternative landing sites. Feasibility and safety guarantees of the proposed approach are discussed in Section IV, and we provide implementation details and the divert-feasible PDG algorithm in Section V. In Section VI, we validate our algorithm on numerical examples for satisfaction of all PDG problem constraints under navigational uncertainty, as well as compute maximum achievable divert distances based on the stochastic controllable sets. Finally, concluding remarks and directions for future work are discussed in Section VII.

II. Problem Description

We use the following notion throughout the paper: $\mathbb{R}$, $\mathbb{R}_+$, $\mathbb{R}^n$, $\mathbb{N}$, are the sets of real numbers, positive real numbers, the Euclidean space, and natural numbers, respectively. The ith row of matrix M is denoted by $[M]_i$. Euclidean distance is denoted by $\|\cdot\|$. A reference frame, $\mathrm{F_x}$ consists of three orthonormal dextral basis vectors $\{\hat{\imath}_\mathrm{x}, \hat{\jmath}_\mathrm{x}, \hat{k}_\mathrm{x}\}$, where $\hat{\cdot}$ denotes a unit vector. The angular velocity vector of frame $\mathrm{F_x}$ with respect to $\mathrm{F_y}$ is denoted by $\omega_{\mathrm{x/y}}$, and $\omega^\times$ denotes the skew-symmetric matrix of ω.

A. Lander dynamics and measurement model

Consider a lander in the powered descent phase to the lunar surface, a non-inertial surface-fixed frame $\mathrm{F_s}$, and an

[1]Department of Engineering Science, University of Oxford, OX1 3PJ, UK; Y. Lishkova interned at MERL during the development of this work.
[2]Mitsubishi Electric Research Laboratories (MERL), MA, 02139, USA
*Corresponding author, weiss@merl.com

inertial frame $\mathrm{F_i}$. The lander is assumed to be rigid and all external forces acting on the lander are modeled as acting on its center of mass. The translation-only dynamics of the lander relative to and resolved in the surface-fixed frame $\mathrm{F_s}$, and its mass depletion dynamics, are given by

$$\ddot{r}(t) = \frac{T_\mathrm{c}(t)}{m(t)} + g - \omega_{\mathrm{s/i}}^{\times}\omega_{\mathrm{s/i}}^{\times} r(t) - 2\omega_{\mathrm{s/i}}^{\times}\dot{r}(t), \tag{1a}$$

$$\dot{m}(t) = -\|T_\mathrm{c}(t)\|/g_\mathrm{e} I_\mathrm{sp} = -\beta\|T_\mathrm{c}(t)\|, \tag{1b}$$

where $x = \begin{bmatrix} r^\intercal & \dot{r}^\intercal \end{bmatrix}^\intercal \in \mathbb{R}^6$ is the translational state of the lander, $T_\mathrm{c} \in \mathbb{R}^3$ is the net thrust applied to the lander, $g \in \mathbb{R}^3$ is the constant gravity vector of the Moon, $\omega_{\mathrm{s/i}}$ is the Moon's constant angular velocity vector with respect to the inertial frame $\mathrm{F_i}$, $m \in \mathbb{R}_+$ is the mass of the lander, $g_\mathrm{e} \in \mathbb{R}_+$ is Earth's standard gravitational acceleration, and $I_\mathrm{sp} \in \mathbb{R}_+$ is the specific impulse of the lander's engine.

Uncertainty model: During powered descent, the lander does not have access to its true position and velocity. We model this navigational uncertainty as noisy state estimates $y(t) \in \mathbb{R}^6$ such that

$$y(t) = x(t) + \nu(t), \tag{2}$$

where $\nu(t) \sim \mathcal{N}(0, \Sigma_\nu)$ is an independent and identically distributed Gaussian noise that models the state estimate uncertainty with zero mean and known covariance matrix $\Sigma_\gamma \in \mathbb{R}^{6\times 6}$.

B. PDG constraints

The lander is limited by physical and operational constraints given by [6],

$$m_\mathrm{d} \le m(t) \le m_\mathrm{w}, \tag{3a}$$

$$\rho_1 \le \|T_\mathrm{c}(t)\| \le \rho_2, \tag{3b}$$

$$\|T_\mathrm{c}(t)\|\cos(\theta_\mathrm{max}) \le \hat{n}^\intercal T_\mathrm{c}(t), \tag{3c}$$

$$\|r(t) - r_\mathrm{ls}\|\cos(\gamma) \le \hat{k}_\mathrm{s}^\intercal r(t), \tag{3d}$$

$$\|\dot{r}(t)\| \le v_\mathrm{max}. \tag{3e}$$

Constraint (3a) requires that the lander's mass lie between the dry mass m_d and wet mass $m_\mathrm{w} = m_\mathrm{d} + m_\mathrm{f}$, where m_f is the initial mass of the available fuel. Constraint (3b) requires that the thrust is bounded from above and below with known constants ρ_1, ρ_2. Constraint (3c) is an attitude constraint that limits the thrust vector from deviating by more than $\theta_\mathrm{max} \in [0, \pi]$ from a pre-specified direction $\hat{n} \in \mathbb{R}^3$, and is often used to either limit the tilt angle of the lander from the vertical, or ensure sensor line of sight with the landing target. Constraint (3d) is a glideslope constraint with glideslope angle $\gamma \in [0, \pi/2]$ relative to landing site $r_\mathrm{ls} \in \mathbb{R}^3$, such that the lander can avoid crashing into nearby terrain. Finally, constraint (3e) sets a maximum velocity $v_\mathrm{max} \in \mathbb{R}$.

C. Fuel-optimal PDG under navigational uncertainty

We wish to drive the true state of the lander with uncertain initial conditions

$$x(0) \sim \mathcal{N}(y(0), \Sigma_\nu), \qquad m(0) = m_\mathrm{w}, \tag{3f}$$

where $y(0)$ is the noisy state estimate at the start of the powered descent, to a convex and compact region $\mathcal{X}_\mathrm{ls} \subset \mathbb{R}^6$ around a landing site $r_\mathrm{ls} \in \mathbb{R}^3$, such that

$$x(t_\mathrm{f}) \in \mathcal{X}_\mathrm{ls}. \tag{3g}$$

To do so, we formulate the fuel-optimal PDG optimal control problem (OCP) under navigational uncertainty as

$$\min_{t_\mathrm{f}, T_\mathrm{c}} \left(m(0) - m(t_\mathrm{f})\right) \text{ s.t. } \forall t \in [0, t_\mathrm{f}]$$

$$\text{Dynamics (1) with initial conditions (3f),} \tag{4a}$$

$$\mathbb{P}\{\text{constraints (3a)-(3e),(3g) are satisfied}\} \ge \alpha. \tag{4b}$$

In (4), $\alpha \in (0, 1]$ is a probability threshold selected to ensure that the constraints (3a)-(3e), (3g) are met with a likelihood no smaller than α.

We seek a tractable method to solve (4) and to leverage that method to divert to an alternative landing site in case a hazard is detected.

Problem 1 (Nominal trajectory design): Design a tractable optimization formulation of (4) for constraint-admissible PDG under navigational uncertainty with greater than or equal to user-specified probability.

Problem 2 (Hazard avoidance): If a hazard is detected, identify a reachable, alternative landing site and use a modified version of (4) to divert to the selected site.

III. Proposed Approach

To solve Problem 1, we reformulate (4) as a convex chance-constrained optimal control problem, given by OCP 1 in Section III-A.3. To solve Problem 2, we develop inner-approximations of stochastic controllable sets, which characterize the sets of noisy state estimates from which the lander can be driven to a landing site with user-specified probability using OCP 2 and OCP 3 in Section III-B. The stochastic controllable sets enable a real-time assessment of the reachability of alternative landing sites.

A. Convex chance-constrained PDG

1) Model reformulation: Let $u(t) \triangleq \frac{T_\mathrm{c}(t)}{m(t)}$, then the translational dynamics (1a) can be written as

$$\dot{x}(t) = Ax(t) + Bu(t) + G, \tag{5}$$

for appropriate A, B, G matrices. We reformulate the initial-time Gaussian noise $\nu(0)$ as a state disturbance that with probability α lies in the ellipsoid

$$\mathcal{E}_\alpha : \{\nu(0) \mid \nu(0)^\intercal \Sigma^{-1} \nu(0) \le F^{-1}_{\chi^2(6)}(\alpha)\}, \tag{6}$$

that is, $\mathbb{P}\{\nu(0) \in \mathcal{E}_\alpha\} = \alpha$, where $\chi^2(6)$ is a chi-squared random variable with six degrees of freedom, and $F_{\chi^2(6)}(\cdot)$ is its cumulative distribution function [14]. Given an estimate $y(0)$, the ellipsoid $\mathcal{X}(0) = \{y(0)\} \oplus \mathcal{E}_\alpha$ contains all possible true initial states $x(0)$ with probability α by (3f). The evolution of the possible true trajectories $x(t)$ evolving from $\mathcal{X}(0)$ is given by

$$x(t) \in \mathcal{X}(t) : \{x \mid (\bar{x}(t) - x)^\intercal S(t) (\bar{x}(t) - x) \le 1\}, \tag{7a}$$

$$S(t) = \Phi(0,t)S(0)\Phi(0,t)^\intercal, \quad S(0) = \frac{1}{R^2}\Sigma^{-1}, \tag{7b}$$
$$\dot{\bar{x}}(t) = A\bar{x}(t) + Bu(t) + G, \quad \bar{x}(0) = y(0), \tag{7c}$$

where $R^2 = F^{-1}_{\chi^2(6)}(\alpha)$, and $\Phi(0,t)$ is the state transition matrix for the dynamics defined by (5).

2) Constraint reformulation: Next, the glideslope and maximum velocity constraints (3d), (3e) are replaced by conservatively substituting their ℓ^2-norms with ℓ^∞/ℓ^1-norms. The resulting affine constraints can be written compactly as

$$H(\bar{x}(t) - x_{\rm ls}) \leq f, \tag{8}$$

where the matrix of normals $H \in \mathbb{R}^{6\times n_{\rm H}}$ and the vector of facet offsets $f \in \mathbb{R}^{n_{\rm H}}$ define a polytopic constraint set [6]. To ensure the tube of possible trajectories $\mathcal{X}(t)$ remains feasible, we tighten constraint (8) using [15]

$$\|S(t)^{1/2}[H]_i\| \leq -[H]_i(\bar{x}(t) - x_{\rm ls}) + [f]_i \;\; i = 1, ..., n_H. \tag{9}$$

Additionally, (3g) is replaced with

$$\bar{x}(t_{\rm f}) = \bar{x}^*_{t_{\rm f}}, \tag{10}$$

$$\text{where: } \bar{x}^*_{t_{\rm f}} = \arg\min_{\bar{x}_{t_{\rm f}}} (\bar{x}_{t_{\rm f}} - x_{\rm ls})^\intercal(\bar{x}_{t_{\rm f}} - x_{\rm ls}), \tag{11a}$$
$$\text{s.t. } \|S(t_{\rm f})^{1/2}[H]_i\| \leq -[H]_i(\bar{x}_{t_{\rm f}} - x_{\rm ls}) + [f]_i. \tag{11b}$$

Problem (11) finds the closest possible final state $\bar{x}(t_{\rm f})$ to the desired landing location $x_{\rm ls}$ such that the set of possible true states $\mathcal{X}(t_{\rm f})$ fits in the polytope (9).

3) Lossless convexification: Substituting (7b), (7c) for (1a), (9) for (3d), (3e), and (10) for (3g), the OCP in (4) can be transformed into a convex problem using lossless convexification techniques [6]–[9]. Following [7], dynamics (1b) and constraints (3a), (3b), (3c) become

$$\dot{z} = -\beta\sigma(t) \tag{12}$$
$$z^0(t) \leq z(t) \leq \ln(m_{\rm w} - \beta\rho_1 t), \quad z(0) = \ln(m_{\rm w}), \;\; \ln(m_{\rm d}) \leq z(t_{\rm f}), \tag{13a}$$
$$\rho_1 e^{-z^0(t)}[1 - (z(t) - z^0(t)) + \tfrac{(z(t)-z^0(t))^2}{2}] \leq \sigma(t), \tag{13b}$$
$$\sigma(t) \leq \rho_2 e^{-z^0(t)}[1 - (z(t) - z^0(t))], \tag{13c}$$
$$\hat{n}^\intercal u(t) \geq \sigma(t)\cos(\theta_{\max}), \tag{13d}$$
$$\|u(t)\| \leq \sigma(t), \tag{13e}$$

where $z(t) \triangleq \ln(m(t))$, $z^0(t) = \ln(m_{\rm w} - \beta\rho_2 t)$, and $\sigma(t)$ is a slack variable used in the convexification process. With these substitutions, we formulate

OCP 1: $\max_{u,\sigma,t_{\rm f}} z(t_{\rm f})$ subject to $\forall t \in [0, t_{\rm f}]$
dynamics (7b), (7c), (12), constraints (9),(10),(13).

As will be proven in Section IV, OCP 1 is a tractable chance-constrained formulation of (4) and solves Problem 1.

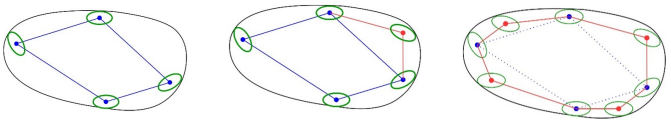

Fig. 1: Illustration of the computation procedure for $\tilde{\mathcal{C}}(m^{\rm s}_{\rm w})$. L to R: 1) Initial set, 2) Pushing along a face, 3) Result.

B. Divert-feasible sets

During powered descent, planetary landers scan the terrain for hazards and produce candidate landing sites. If a hazard is detected at the nominal landing site $r_{\rm ls}$, the lander needs to quickly identify which alternatives are reachable. Since solving OCP 1 to each candidate site may be too computationally intensive, we compute offline a database of polytopic stochastic controllable sets parameterized by mass $m^{\rm s}_{\rm w} \in [m_{\rm d}, m_{\rm w}]$. The stochastic controllable sets characterize the set of noisy state estimates from which the lander can be driven to a specified landing site with user-specified probability. Online, the current state estimate of the lander is checked for inclusion against the database of sets at candidate sites. The inclusion check amounts to either evaluating linear inequalities if a halfspace representation of the set is known or a linear program in the case of a vertex representation.

For tractability, we combine the approach of [11] with the reformulation of Section III-A, to compute robust controllable set-based inner approximations of the stochastic controllable sets. To aid the discussion, we define the feasible set by the convexified dynamics (5), (12), and constraints (8), (13), in the absence of navigational uncertainty

$$\text{Feas}(m^{\rm s}_{\rm w}) \triangleq \left\{ (x(0), u) \;\middle|\; \begin{array}{c} \exists t_{\rm f} \geq 0 \text{ s.t. } \forall t \in [0, t_{\rm f}], \\ (x(t), u(t)) \text{ satisfies} \\ \text{(3g), (5), (8), (12), (13)} \end{array} \right\}. \tag{15}$$

In the presence of navigational uncertainty, we define the stochastic controllable set as a set-valued function of $m^{\rm s}_{\rm w}$

$$\begin{aligned} \mathcal{C}(m^{\rm s}_{\rm w}) \triangleq \{y(0) : \exists u \text{ s.t.} \\ \mathbb{P}_{\nu(0)}\{(y(0) - \nu(0), u) \in \text{Feas}(m^{\rm s}_{\rm w})\} \geq \alpha\}, \end{aligned} \tag{16}$$

with $x_{\rm ls} = 0$, which, for a given $m^{\rm s}_{\rm w}$, is the set of all initial state estimates $y(0)$ for which there exists a constraint-admissible control sequence that drives the lander to the origin with at least probability α. Note that with $x_{\rm ls} = 0$, the constraints in (16) are, and thus the set $\mathcal{C}(m^{\rm s}_{\rm w})$ is, invariant under translation.

Analogous to [11], the inner approximation of each set $\mathcal{C}(m^{\rm s}_{\rm w})$ is constructed in several stages. First, we formulate a set of convex programs

OCP 2: For i = 1,....,12
$\max_{\bar{x}(0),u,t_{\rm f}} \; [[\bar{x}(0)^\intercal, -\bar{x}(0)^\intercal]^\intercal]_i$ subject to for $\forall t \in [0, t_{\rm f}]$
dynamics (7b), (7c), (12), constraints (9), (10), (13).

OCP 2 finds the extreme points $\bar{x}(0) \in \mathcal{C}(m^{\rm s}_{\rm w})$ for which the corresponding ellipsoidal set of possible true initial states $\mathcal{X}(0)$ can be driven to the origin (proof in Section IV). The

Algorithm 1: Computation of $\tilde{\mathcal{C}}(m_{\mathrm{w}}^s)$

Input :

n_{sets} and $m_{\mathrm{w}}^{\mathrm{s}}$ for $s = 0, ..., n_{\mathrm{sets}}$;

Offline:

for $s = 0, ..., n_{\mathrm{sets}}$: **do**
  solve OCP 2 with $m_{\mathrm{w}} = m_{\mathrm{w}}^{\mathrm{s}}$ to create $\tilde{\mathcal{C}}(m_{\mathrm{w}}^s)$;
  iter = 1;
  while *iter*$<$ $maxiter_{\mathrm{sets}}$ **do**
    $iter = iter + 1$;
    solve OCP 3 to enlarge $\tilde{\mathcal{C}}(m_{\mathrm{w}}^s)$

convex hull of the resulting twelve $\bar{x}(0)$ points $\tilde{\mathcal{C}}(m_{\mathrm{w}}^s)$ is taken as the initial approximation of $\mathcal{C}(m_{\mathrm{w}}^{\mathrm{s}})$. In the next step, the sets are enlarged by finding the outward normal $\hat{n}_{\mathrm{facet},i}$ to each of the polytope facets and finding the furthest point $\bar{x}(0)$ from the facet for which all points in the corresponding set $\mathcal{X}(0)$ remain as feasible initial conditions. This procedure is achieved by solving

OCP 3: For $i = 1, ..., n_{\mathrm{facets}}$

$$\max_{\bar{x}(0),u,\sigma,t_{\mathrm{f}}} \ \hat{n}_{\mathrm{facet},i}^{\intercal}\bar{x}(0) \ \text{ subject to for } \forall t \in [0, t_{\mathrm{f}}]$$

dynamics (7c), (12), constraints (7b), (9), (10), (13).

In OCP 3, n_{facets} is the number of facets of $\tilde{\mathcal{C}}(m_{\mathrm{w}}^s)$. The resulting points $\bar{x}(0)$ are added to the set of vertices of $\tilde{\mathcal{C}}(m_{\mathrm{w}}^s)$, and the convex hull is updated. The resulting polytope $\tilde{\mathcal{C}}(m_{\mathrm{w}}^s)$ can again be enlarged in the same way, facet by facet. As suggested in [11], this iteration can be stopped based on the available computational resources or a tolerance on the volume difference between $\tilde{\mathcal{C}}(m_{\mathrm{w}}^s)$ and an an outer approximation. The final $\tilde{\mathcal{C}}(m_{\mathrm{w}}^s)$ thus approximates the $\mathcal{C}(m_{\mathrm{w}}^{\mathrm{s}})$ set and the overall proposed procedure is written in Algorithm 1 and depicted graphically for an example 2D set in Fig. 1.

In Section IV, we prove that $\tilde{\mathcal{C}}(m_{\mathrm{w}}^s)$ is a subset of the $\mathcal{C}(m_{\mathrm{w}}^{\mathrm{s}})$ for the given m_{w}^s, regardless of the number of enlarging iterations. That is, given a control sequence u obtained using OCP 1 for an initial point $y_0 \in \tilde{\mathcal{C}}(m_{\mathrm{w}}^s)$, then u will drive all points $x_0 \in \{y_0\} \oplus \mathcal{E}_\alpha$ to the landing location safely with a probability α or higher, i.e $\mathbb{P}((y_0, u) \in \mathrm{Feas}(m_{\mathrm{w}}^{\mathrm{s}})) \geq \alpha$. Most importantly, we can prove that $\tilde{\mathcal{C}}(m_{\mathrm{w}}^s)$ is an inner approximation of the stochastic controllable set for this mass and the original nonlinear dynamics.

Remark 1: Notably, the $\tilde{\mathcal{C}}(m_{\mathrm{w}}^s)$ sets are six-dimensional. The lander mass was not taken as a degree of freedom as the resulting set computation problem would be nonconvex.

IV. Feasibility and Safety Guarantees

We first prove that the computed $\tilde{\mathcal{C}}(m_{\mathrm{w}}^s)$ sets using Algorithm 1 are inner approximations of the corresponding $\mathcal{C}(m_{\mathrm{w}}^{\mathrm{s}})$. Then we show that the control sequence obtained by solving OCP 1 drives all trajectories evolving from the ellipsoid of possible true initial states to the landing site without violating the system or control constraints. The same control sequence drives any possible true initial state in the assumed Gaussian distribution to the landing site without violating system and control constraints with probability at least α.

A. Stochastic controllable sets

In Section III-B, we defined the $\mathcal{C}(m_{\mathrm{w}}^{\mathrm{s}})$ set. Using the definitions (6), (7) a tractable alternative set can be defined as

$$\mathcal{Y}(m_{\mathrm{w}}^s) \triangleq \{y(0) : \exists u \ \text{ for } \forall \nu(0) \in \mathcal{E}_\alpha \text{ s.t } (y(0) - \nu(0), u) \in \mathrm{Feas}(m_{\mathrm{w}}^{\mathrm{s}})\}. \tag{19}$$

Lemma 1: $\mathcal{Y}(m_{\mathrm{w}}^s) \subseteq \mathcal{C}(m_{\mathrm{w}}^{\mathrm{s}})$

Proof: Let $y \in \mathcal{Y}(m_{\mathrm{w}}^s)$. From (6), (7) and (19) it follows

$$\mathbb{P}\{(y(0) - \nu(0), u) \in \mathrm{Feas}(m_{\mathrm{w}}^{\mathrm{s}}) |\, \nu(0) \in \mathcal{E}_\alpha\} = 1. \tag{20}$$

Consequently,

$$\begin{aligned}&\mathbb{P}_{\nu(0)}\{(y(0) - \nu(0), u) \in \mathrm{Feas}(m_{\mathrm{w}}^{\mathrm{s}})\} \geq \\ &\mathbb{P}_{\nu(0)}\Big\{(y(0) - \nu(0), u) \in \mathrm{Feas}(m_{\mathrm{w}}^{\mathrm{s}})\} \cap \{\nu(0) \in \mathcal{E}_\alpha\}\Big\} = \\ &\mathbb{P}\{(y(0) - \nu(0), u) \in \mathrm{Feas}(m_{\mathrm{w}}^{\mathrm{s}}) |\, \nu(0) \in \mathcal{E}_\alpha\}\mathbb{P}\{\nu(0) \in \mathcal{E}_\alpha\} = \alpha.\end{aligned} \tag{21}$$

Thus from (16), $y(0) \in \mathcal{C}(m_{\mathrm{w}}^{\mathrm{s}})$. □

Lemma 2: Let $(u^*, \sigma^*, t_{\mathrm{f}}^*)$ be the solution of OCP 2 (OCP 3) for a given m_{w} and initial state estimate $y(0) \in \mathcal{Y}(m_{\mathrm{w}}^s)$. Then, at all temporal nodes, the trajectory starting from any point $x_0 \in \mathcal{X}(0)$ under the guidance u^* satisfies the constraints forming the feasibility set $\mathrm{Feas}(m_{\mathrm{w}}^{\mathrm{s}})$,

$$(x_0, u^*) \in \mathrm{Feas}(m_{\mathrm{w}}^{\mathrm{s}}) \ \forall x_0 \in \mathcal{X}(0).$$

Proof: The tightened constraint (9) can be generalized at all discrete temporal nodes as

$$[H]_i \bar{x}_k + \mathrm{Support}_{\mathrm{Reach}(k,\mathcal{E}_\alpha)}([H]_i) \leq [f]_i, \tag{22}$$

for $i = 1, ..., n_H$ where $\mathrm{Support}_R(l) = \max_{\zeta \in R} l^{\intercal}\zeta$ and

$$\mathrm{Reach}(k, \mathcal{E}_\alpha) = \left\{ \prod_{t=0}^{k-1} A_d^t \nu(0) \mid \nu(0) \in \mathcal{E}_\alpha \right\}.$$

From the superposition principle, due to linearity of (5), $x(t) = \bar{x}(t) + \nu(t)$, where $\nu(t) \in \Phi(0, t)\mathcal{E}_\alpha$. Similarly, at the temporal nodes, $x_k = \bar{x}_k + \nu_k$, where $\nu_k \in \mathrm{Reach}(k, \mathcal{E}_\alpha)$. Thus, from the tightening of the constraints (22), it follows that $Hx_k \leq f$. □

Corollary 1: Lemma 2 holds for a given landing location x_{ls}. Due to the assumption that the constraints (9), (13) are invariant with respect to translation, the sets can be translated to new landing locations without loss of safety guarantees when landing at the newly chosen landing site.

Theorem 1: $\tilde{\mathcal{C}}(m_{\mathrm{w}}^s)$, computed using Algorithm 1, is an inner-approximation to $\mathcal{C}(m_{\mathrm{w}}^{\mathrm{s}})$.

Proof: Let q_i be the i-th vertex of $\tilde{\mathcal{C}}(m_{\mathrm{w}}^s)$ computed in step 2 or 6 in Algorithm 1. From Lemma 2 it follows that $(\{q_i\} \oplus \mathcal{E}_\alpha, u) \subseteq \mathrm{Feas}(m_{\mathrm{w}}^{\mathrm{s}})$ thus $q_i \in \mathcal{Y}$. Given that $\tilde{\mathcal{C}}(m_{\mathrm{w}}^s)$ is the convex hull of $\{q_i\}$ and $\mathcal{Y}(m_{\mathrm{w}}^s)$ is also convex, it

follows $\tilde{\mathcal{C}}(m_{\mathrm{w}}^s) \subseteq \mathcal{Y}(m_{\mathrm{w}}^s)$ and from Lemma 1 it follows that $\tilde{\mathcal{C}}(m_{\mathrm{w}}^s) \subseteq \mathcal{C}(m_{\mathrm{w}}^s)$. □

The sets $\tilde{\mathcal{C}}(m_{\mathrm{w}}^s)$ are defined from the convexified problem.

Theorem 2: $\tilde{\mathcal{C}}(m_{\mathrm{w}}^s)$ is an inner approximation for a stochastic controllable set defined using the feasibility set (15) with the nonlinear dynamics and constraints (1b), (3) replacing (12),(13).

Proof (sketch): The proof follows from Theorem 1, the convexity of the sets $\tilde{\mathcal{C}}(m_{\mathrm{w}}^s)$ and the fact that each of the vertices of these set, computed using OCP 2 or 3, is guaranteed to be reachable for the original nonlinear dynamics based on proofs from [16] and Section II.C in [11], respectively.

B. Stochastic trajectory optimization:

Based on the formulation of OCP 1, 2, and 3, one can make the following statement:

Lemma 3: Let $(u^*, \sigma^*, t_{\mathrm{f}}^*)$ be the solution of OCP 1 for a given m_{w} and an initial state measurement $y_0 \in \mathcal{Y}(m_{\mathrm{w}}^s)$. Then at all temporal nodes, the trajectory starting from any point $x_0 \in \{y(0)\} \oplus \mathcal{E}_\alpha$ under the guidance u^* satisfies the constraints of OCP 1,2, and 3, i.e.

$$\mathbb{P}\{(x_0, u^*) \in \text{Feas}(m_{\mathrm{w}}^{\mathrm{s}})\} = 1,$$

For a general $\nu(0)$ from the considered Gaussian distribution and the corresponding true state $x_0 = y_0 + \nu_0$ it holds that

$$\mathbb{P}\{(x_0, u^*) \in \text{Feas}(m_{\mathrm{w}}^{\mathrm{s}})\} \geq \alpha. \tag{23}$$

Proof: The proof is analogous to the proof of Lemma 1 and (23) follows from Equation (21). □

In other words, the control trajectory u^* obtained using OCP 1 drives all trajectories started from the ellipsoid of possible initial true states $X_0 = \{y(0)\} \oplus \mathcal{E}_\alpha$ to the landing location safely without violating any constraints. Because $\mathbb{P}(\nu(0) \in \mathcal{E}_\alpha) = \alpha$, it follows that for a general $\nu(0)$ from the considered distribution, and its associated true state $x(0)$, landing is achieved without violating the constraints with a probability of α or higher. Thus, OCP 1 achieves the goals set out in (4) and Problem 1.

V. Implementation

OCP 1, OCP 2, and OCP 3 can be discretized and solved numerically analogously to the lossless convexification approach in [6].

Remark 2: In the discrete-time case, the OCP problems are solved with a fixed final time t_{f}. The optimal t_{f}^* can be found by implementing a golden search algorithm that solves OCP 1 repeatedly for $t_{\mathrm{f}} \in [0, \bar{t}_{\mathrm{f}}]$ for the maximum z_N^*. A guess on the upper bound $\bar{t}_{\mathrm{f}}$ can be made heuristically to $\bar{t}_{\mathrm{f}} = m_{\mathrm{w}}/(\beta\rho_2)$ using $z_N^0 = \ln(m_{\mathrm{w}} - \beta\rho_2 N\Delta t)$. If OCP 1 is infeasible in the range $[0, \bar{t}_f]$, we set z_N for that t_{f} value as very large to guide the search toward feasible regions. The same check is done for values above $\bar{t}_{\mathrm{f}}$. The upper bound is adjusted if feasible solutions are found. This procedure for finding t_{f}^* is inspired by the deterministic studies in [9] and [17] based on the unimodality of the $m_{\mathrm{f,used}}$ function with respect to t_{f}.

Analogously to the computation of $\tilde{\mathcal{C}}(m_{\mathrm{w}}^s)$, in discrete time, the time-discretized OCP 2 and 3 lead to the formulation of the set $\tilde{\mathcal{D}}(m_{\mathrm{w}}^s, t_{\mathrm{f}}^s)$. In practice $\tilde{\mathcal{D}}(m_{\mathrm{w}}^s, t_{\mathrm{f}}^s)$ sets can be computed offline for a countable number n_{pairs} of pairs $(m_{\mathrm{w}}^{\mathrm{s}}, t_{\mathrm{f}}^{\mathrm{s}})$ and used during hazard avoidance, as will be demonstrated in Algorithm 2.

Remark 3: As suggested by [11], for numerical reasons, the parameter scaling can be chosen for time-discretized OCP 1, 2, and 3 based on a single computation of time-discretized OCP 2 which maximizes only $i = 1, 2, 3, 7, 8, 9$.

Remark 4: Similar guarantees to those in Section IV-A for the continuous setting can be proven for the discrete sets computed by Algorithm 2, offline. In the discrete-time case, we can similarly define, based on the time-discretized and convexified constraints in the absence of navigational uncertainty, the set $\mathcal{D}(m_{\mathrm{w}}^s, t_{\mathrm{f}}^s)$ as the discrete-time analogy of the $\mathcal{C}(m_{\mathrm{w}}^{\mathrm{s}})$ set but sliced for a given t_{f}^s. Analogously to the proofs of Lemma 1 and Theorem 1, it can then be shown that $\tilde{\mathcal{D}}(m_{\mathrm{w}}^s, t_{\mathrm{f}}^s)$, computed by Algorithm 2, offline, is an inner-approximation to $\mathcal{D}(m_{\mathrm{w}}^s, t_{\mathrm{f}}^s)$. Furthermore, the same guarantees as those presented in Section IV-B can be formulated for the control sequence resulting from the time-discretized problem formulation.

A. Divert-feasible PDG

The summary of the approach for the numerical solution of Problems 1 and 2 is presented in Algorithm 2.

Remark 5: One can easily obtain the maximum divert distance achievable by solving online a linear program for each of the pre-computed $\tilde{\mathcal{D}}(m_{\mathrm{w}}^s, t_{\mathrm{f}}^s)$ sets and determining for what shift the given trajectory point remains in the convex hull of the selected set. The linear program is given by

$$\max_{\mathbf{w}} \Delta r_{\mathbb{x}} \;\text{ s.t. : } \begin{bmatrix} V^{\intercal} \\ \mathbf{1} \end{bmatrix} \mathbf{w} = \begin{bmatrix} y_h \\ 1 \end{bmatrix} + \begin{bmatrix} \Delta r_{\mathbb{x}} \\ \mathbf{0} \end{bmatrix}, \; \mathbf{w} \geq \mathbf{0}, \tag{24}$$

where $V \in \mathbb{R}^{n_v \times 6}$ is a matrix of stacked points defining the convex hull of the selected set, y_h is the measured x at the time of hazard detection, $\mathbf{1}$ is a vector of ones, and $\mathbf{0}$ a vector of 0's. While the linear program (24) finds the maximum shift along the x-axis, it can trivially be adjusted for alternative directions. Only $\tilde{\mathcal{D}}(m_{\mathrm{w}}^s, t_{\mathrm{f}}^s)$ sets with m_{w}^s smaller than the current mass of the spacecraft should be tested.

VI. Results

The proposed method was implemented in Python using the cvxpy library [18] with the CLARABEL solver [19]. Parameters used for all simulations are tabulated in Table I. The $\tilde{\mathcal{C}}(m_{\mathrm{w}}^s)$ sets are calculated with $maxiter_{\mathrm{sets}}$ iterations. The stochastic model is created using 3σ calculation based on zero mean and scaled deviations $3\sigma([\nu_0]_{[1:3]})$, $3\sigma([\nu_0]_{[4:6]})$.

A. Validating the set computations

To verify the construction of $\tilde{\mathcal{D}}(m_{\mathrm{w}}^s, t_{\mathrm{f}}^s)$ proposed in Algorithm 2, we demonstrate the validity of Lemma 2. We perform the test with $m_{\mathrm{w}}^s = m_{\mathrm{w}} = 1300$kg, $t_{\mathrm{f}} = 90$s, and $maxiter_{\mathrm{sets}} = 3$. Let $\bar{\mathbf{x}}^* = \{\bar{x}_0^*, ..., \bar{x}_N^*\}$, $\mathbf{u}^* = \{u_0^*, ..., u_{N-1}^*\}$ represent the center trajectory and controls

Algorithm 2: Divert-feasible PDG under navigational uncertainty

Input :

x_{ls}, n_{pairs} and $(m_{\text{w}}^{\text{s}}, t_{\text{f}}^{\text{s}})$ for $s = 0, ..., n_{\text{pairs}}$;

Offline: Obtain a database of $\tilde{\mathcal{D}}(m_{\text{w}}^{s}, t_{\text{f}}^{s})$ applicable to any landing location

for $s = 0, ..., n_{\text{pairs}}$: **do**
  solve the time-discretized OCP 2 with $m_{\text{w}} = m_{\text{w}}^{\text{s}}, t_{\text{f}} = t_{\text{f}}^{\text{s}}$ to create $\tilde{\mathcal{D}}(m_{\text{w}}^{s}, t_{\text{f}}^{s})$;
  iter = 1;
  while *iter*$<$ $maxiter_{\text{sets}}$ **do**
    $iter = iter + 1$;
    solve the time-discretized OCP 3 to enlarge $\tilde{\mathcal{D}}(m_{\text{w}}^{s}, t_{\text{f}}^{s})$

Online:

Measure y_0 ;
Find t_{f}^{*} as suggested by Remark 2;
Solve the time-discretized OCP 1 to obtain $u_0, .., u_{N-1}$;
for $k = 0, ..., N-1$ **do**
  Check for hazard ;
  if *hazard* **then**
    safe = False ;
    $N - k \to N, 0 \to k$;
    while *safe* = *False* **do**
      Choose a different landing site x_{ls}^{new};
      while $s \in [0, n_{\text{pairs}}]$ *and safe*=*False* **do**
        Measure y_0;
        if $y_0 \in \tilde{\mathcal{D}}(m_{\text{w}}^{s}, t_{\text{f}}^{s})$ **then**
          safe=True;
          solve the time-discretized OCP 1 with $x_{\text{ls}}^{new} \to x_{\text{ls}}$, to obtain new $u_0, ..., u_{N-1}$
  Implement u_k ;

obtained by the solution of the time-discretized OCP 1 from an extreme point $q \in \tilde{\mathcal{D}}(m_{\text{w}}^{s}, t_{\text{f}}^{s})$. We perform a Monte Carlo simulation, picking possible true initial points $x_0^{\{j\}} \in \{q\} \oplus \mathcal{E}_{\alpha}$ and obtaining forward simulation trajectories $\mathbf{x}^{\{j\}} = \{x_0^{\{j\}}, ..., x_N^{\{j\}}\}$ using (7c), (12) discretized with a first order holder from q under u^*. We do this for 100 points. Fig. 2 demonstrates the $\tilde{\mathcal{D}}(m_{\text{w}}^{s}, t_{\text{f}}^{s})$ set for the given landing location, the center trajectory, and the tube of $\mathbf{x}^{\{j\}}$ trajectories. Fig. 3a shows that all trajectories reach the desired landing zone, and from numerical simulations, they all respected the constraints of the original nonlinear problem. All other nonlinear constraints for the original problem were also satisfied for all the trajectories in the bundle. For comparison, the same Monte Carlo test under initial state uncertainty of the extreme points of the deterministic set calculation proposed in [11] was performed again from a random vertex of the set, and as can be seen in Fig. 3b, the

Moon & Lander parameters		Constraints specifications	
g	$[0, 0, -1.62]^{\intercal} m/s^2$	$x_{\text{ls}}^{\text{nominal}}$	$[0, 0, 0, 0, 0, 0]^{\intercal}$
m_{d}	900 kg	$v_{\max}$	300 m/s
ρ_1	1657.27 N	$\theta_{\max}$	25°
ρ_2	4419.39 N	$\hat{n}$	$[0, 0, 1]^{\intercal}$
I_{sp}	255 s	γ	75°
Simulation parameters			
Δt	10 s	$3\sigma([\nu_0]_{[1:3]})$	$[3, 3, 3]^{\intercal}$ m
α	0.7	$3\sigma([\nu_0]_{[4:6]})$	$[0.01, 0.01, 0.01]^{\intercal}$ m/s

TABLE I: Implementation specifications

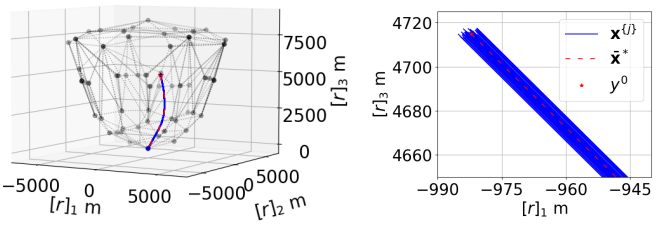

Fig. 2: Simulated trajectory of possible tubes from a chosen vertex point for set verification. Grey - $\tilde{\mathcal{D}}(m_{\text{w}}^{s}, t_{\text{f}}^{s})$, red - $\tilde{\mathbf{x}}^*$, blue - simulated trajectories $\mathbf{x}^{\{j\}}$.

percentage that reach the end goal from a true state around the example vertex was far from 1.

B. Trajectory design and hazard avoidance

We now demonstrate Algorithm 2 capabilities in case of hazard detection for online landing site selection and safe landing. We pre-compute multiple sets with m_{w} and t_{f}, $maxiter_{\text{sets}} = 2$ and, just for simplicity, neglect the maximum velocity constraint. Using the time-discretized OCP 1, we compute an initial trajectory from $m_{\text{w}} = 1300kg$, $t_{\text{f}} = 90s$ to the original landing site $x_{\text{ls}}^{\text{nominal}}$. At each of the discrete steps of this trajectory we assume a hazard has been detected and use (24) to calculate the maximum shift of the landing site it is possible to perform a safe landing with respect to the constraints using the time-discretized OCP 1. This is done by using (24) to compute the maximum shift in which the current trajectory point and mass point belong to a pre-computed $\tilde{\mathcal{D}}(m_{\text{w}}^{s}, t_{\text{f}}^{s})$ set, and the set with the furthest shift is chosen. We calculate this maximum shift as an example for the positive x, y, and $x = y$ directions and compute the hazard-avoidance trajectory to these sites as presented in Figure 4. It must be noted that all these trajectories satisfied the original nonlinear problem constraints.

VII. Conclusions and Future Work

In this work we developed a formulation for fuel-optimal powered descent guidance under navigational uncertainty. We guaranteed that the problem constraints are satisfied to user-specified probability. We reformulated the guidance problem as a convex chance-constrained optimal control problem, where the probability of constraint satisfaction was assured by tightening the constraints with respect to a bounded uncertainty set. We developed inner-approximations

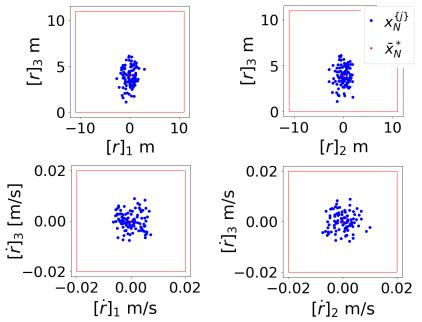

(a) With stochastic computation of the sets

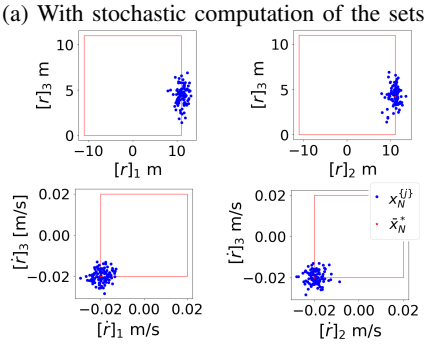

(b) With deterministic computation of the sets

Fig. 3: Degree of success in landing within the desired zone under navigational uncertainty. Red box - chosen landing zone $\mathcal{X}_{\text{ls}}$, red dots - end state for trajectory $\bar{\mathbf{x}}^*$, and blue dots - end state for simulated trajectories $\mathbf{x}^{\{j\}}$.

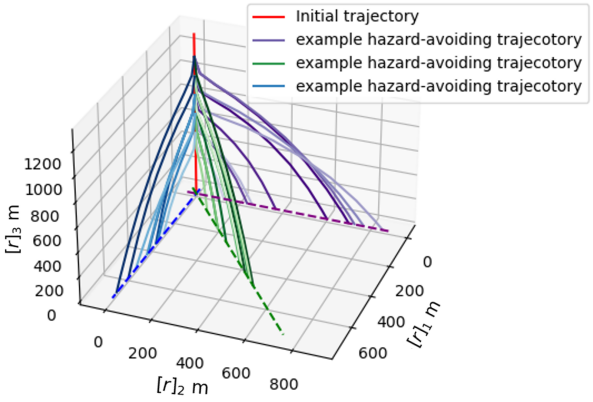

Fig. 4: Hazard avoidance test showing an initial trajectory to a pre-selected landing site and multiple alternative divert trajectories from different stages of the initial trajectory validating divert capabilities in the event of hazard detection.

of stochastic controllable sets that characterized the noisy state estimates from which the lander can be driven to a target with user-specified probability. Using these sets, we developed a divert-feasible powered descent guidance algorithm and demonstrated it on numerical examples. The simulations showed that our problem formulation satisfies the problem constraints despite the navigational uncertainty, successfully landing in the target zone. Finally, we validated the divert-feasible guidance algorithm and simulated maximum achievable divert distances from a nominal trajectory at various altitudes. Future work will extend the development to account for uncertainty in the dynamics.

References

[1] "A Japanese spacecraft faceplanted on the Moon and lived to tell the tale," https://arstechnica.com/space/2024/01/a-japanese-spacecraft-faceplanted-on-the-moon-and-lived-to-tell-the-tale/, accessed: March 17, 2024.

[2] "It turns out that Odysseus landed on the Moon without any altimetry data," https://arstechnica.com/space/2024/02/it-turns-out-that-odysseus-landed-on-the-moon-without-any-altimetry-data/, accessed: March 17, 2024.

[3] M. Anand, "Lunar water: a brief review," *Earth, Moon, and Planets*, vol. 107, pp. 65–73, 2010.

[4] M. Sagliano, "Generalized hp pseudospectral-convex programming for powered descent and landing," *Journal of Guidance, Control, and Dynamics*, vol. 42, no. 7, pp. 1562–1570, 2019.

[5] D. Malyuta, Y. Yu, P. Elango, and B. Açıkmeşe, "Advances in trajectory optimization for space vehicle control," *Annual Reviews in Control*, vol. 52, pp. 282–315, 2021.

[6] D. Malyuta, T. P. Reynolds, M. Szmuk, T. Lew, R. Bonalli, M. Pavone, and B. Açıkmeşe, "Convex optimization for trajectory generation: A tutorial on generating dynamically feasible trajectories reliably and efficiently," *IEEE Control Systems Magazine*, vol. 42, no. 5, pp. 40–113, 2022.

[7] B. Acikmese and S. R. Ploen, "Convex programming approach to powered descent guidance for Mars landing," *Journal of Guidance, Control, and Dynamics*, vol. 30, no. 5, pp. 1353–1366, 2007.

[8] J. M. Carson, B. Açikmeşe, and L. Blackmore, "Lossless convexification of powered-descent guidance with non-convex thrust bound and pointing constraints," in *Proceedings of the 2011 American Control Conference*. IEEE, 2011, pp. 2651–2656.

[9] B. Acikmese, D. Scharf, L. Blackmore, and A. Wolf, "Enhancements on the convex programming based powered descent guidance algorithm for Mars landing," in *AIAA/AAS astrodynamics specialist conference and exhibit*, 2008, p. 6426.

[10] N. Srinivas, A. P. Vinod, S. Di Cairano, and A. Weiss, "Lunar landing with feasible divert using controllable sets," in *AIAA SCITECH 2024 Forum*, 2024, p. 0324.

[11] U. Eren, D. Dueri, and B. Açıkmeşe, "Constrained reachability and controllability sets for planetary precision landing via convex optimization," *Journal of Guidance, Control, and Dynamics*, vol. 38, no. 11, pp. 2067–2083, 2015.

[12] J. Long, A. Gao, and P. Cui, "Controllable set analysis for planetary landing under model uncertainties," *Advances in Space Research*, vol. 56, no. 2, pp. 281–292, 2015.

[13] X. Yuan, Z. Yu, P. Cui, R. Xu, S. Zhu, M. Cao, and E. Luan, "Probability-based hazard avoidance guidance for planetary landing," *Acta Astronautica*, vol. 144, pp. 12–22, 2018.

[14] J. D. Gleason, A. P. Vinod, and M. M. Oishi, "Lagrangian approximations for stochastic reachability of a target tube," *Automatica*, vol. 128, p. 109546, 2021.

[15] S. P. Boyd and L. Vandenberghe, *Convex optimization*. Cambridge university press, 2004.

[16] M. W. Harris and B. Açıkmeşe, "Maximum divert for planetary landing using convex optimization," *Journal of Optimization Theory and Applications*, vol. 162, pp. 975–995, 2014.

[17] L. Blackmore, B. Açikmeşe, and D. P. Scharf, "Minimum-landing-error powered-descent guidance for Mars landing using convex optimization," *Journal of guidance, control, and dynamics*, vol. 33, no. 4, pp. 1161–1171, 2010.

[18] S. Diamond and S. Boyd, "CVXPY: A Python-embedded modeling language for convex optimization," *Journal of Machine Learning Research*, vol. 17, no. 83, pp. 1–5, 2016.

[19] Y. Chen and P. Goulart, "An efficient IPM implementation for a class of nonsymmetric cones," *arXiv preprint arXiv:2305.12275*, 2023.